

1 Computed tomography for iodine contrast media detection using energy information measured by a
2 current-mode detector

3 I. Kanno^{a,*}, R. Imamura^a, K. Mikami^a, M. Ohtaka^b, M. Hashimoto^b, K. Ara^b, H. Onabe^c

4 ^aKyoto University, Sakyo, Kyoto 606-8501, Japan

5 ^bJapan Atomic Energy Agency, O-arai, Ibaraki 311-1393, Japan

6 ^cRaytech Corporation, Yoto, Utsunomiya 321-0904, Japan

7
8 Abstract

9 To exploit the energy information of x-rays in computed tomography (CT), we developed
10 a current-mode detector that gave the energy distribution of the incident x-rays. The CT value
11 obtained for a given material in a phantom depended on the x-ray path length through the phantom.
12 To ensure a constant CT value for a given material, we prepared response functions as a function of
13 the x-rays path length and applied these response functions in the unfolding process. When using
14 response functions that depended on the x-ray path length, the CT values obtained were constant for
15 a given material. In addition, the CT values obtained for iodine contrast media were greater than the
16 values obtained using conventional current CT, especially for higher x-ray tube voltages.

17
18 *Keywords:* Diagnostic X-rays; Unfolding; Energy subtraction method; Contrast media; Filtered
19 X-ray; CT.

20 21 1. Introduction

22
23 X-ray computed tomography (CT) is a powerful method for detecting cancers, especially
24 when they are marked by a contrast media such as iodine. The absorption of x-rays by iodine is
25 *clearly seen above the K-edge of iodine, at 33.2 keV. X-rays with energy much higher than 33.2
26 keV are less effectively absorbed by iodine than for photons with energy 33.2 keV. When the x-ray
27 tube voltage is high and the x-ray energy spectrum is hard, the effect of the iodine contrast media is
28 difficult to observe using the conventional current measurement method. This phenomenon is called
29 the beam hardening effect, and the same effect occurs when a subject is thick. After passing through
30 the thick subject, higher energy x-rays dominate and the absorption effect by iodine is obscured [1].

31 By using information on the x-ray energy, the beam hardening effect can be avoided. As
32 shown in Ref. [2], by exploiting the x-ray events at energies above and below the K-edge of iodine,
33 the absorption effect by iodine is clearly observed, despite the difficulties induced by the x-ray tube
34 voltage and the subject thickness. This method is called energy subtraction (ES) CT.

* Corresponding author. *Tel.:*+81-75-753-5844;*fax.:*+81-75-753-5845.
*E-mail address:*kanno@nucleng.kyoto-u.ac.jp (I.Kanno).

1 The conventional method of measuring x-ray energy, however, takes too long for clinical
2 CT. To make ES CT practical, we invented a new detector that measures x-rays as a current and
3 gives the energy distribution of the x-rays [3]. This detector is called a “transXend” detector. The
4 transXend detector consists of several segment detectors stacked along the direction of x-ray
5 incidence, as shown in Fig. 1. The transXend detector requires a response function to unfold the
6 current data and generate the energy distribution of the incident x-rays. The response function can be
7 obtained using an x-ray simulation code such as EGS5 [4]. It may also be obtained experimentally
8 by measuring x-rays transmitted through several iodine contrast media of known thicknesses.

9 We performed a preliminary CT measurement on a cylindrical acrylic phantom with an
10 iodine region at the center using a transXend detector with CsI(Tl) scintillator segment detectors. ES
11 CT values obtained from the iodine region are much greater than those obtained using conventional
12 current CT [5]. The ES CT values from acrylic regions, however, depended on the acrylic thickness
13 through which the x-rays passed. We did not observe this variation in CT values in the acrylic region
14 when the energy of each x-ray was measured using a conventional CdZnTe detector [2].

15 To ensure that the CT values remain constant for a given material, we prepared response
16 functions for varying thicknesses of the phantom through which the x-rays pass. In this paper, we
17 discuss our method of preparing the response functions and how to apply these response functions in
18 the unfolding method.

19 20 2. Experiment

21 2.1 Experimental setup

22 X-rays were generated by an x-ray tube (TRIX-150S, Toreck Co. Ltd., Japan) and
23 sequentially conditioned using a 2 mm thick Al filter, a Pb collimator (5 mm thick, 5 mm diameter),
24 and a 100 μm thick La filter. In this x-ray beam was placed a rectangular acrylic phantom with four
25 iodine regions filled by thinned iodine tincture with various thicknesses. After transiting the phantom,
26 the x-rays beam was measured using the transXend detector with CsI(Tl) segment detectors, as
27 shown in Fig. 2. The CsI(Tl) segment detectors are made of a CsI(Tl) scintillator array with
28 photodiodes (S5668-11, Hamamatsu Photonics K. K., Japan). The CsI(Tl) scintillators were 2 mm
29 wide, 5 mm high, and 1.175 mm thick. For experiments, the first two photodiodes with scintillators
30 on them were connected together and behaved as a segment detector No. 1. In the same way, we had
31 six segment detectors with twelve CsI(Tl) scintillators and photodiodes. The current measured by
32 the segment detectors was amplified using a six-channel current preamplifier (IPA-6, Raytech Corp.,
33 Japan) and was read out simultaneously using a voltage-frequency converter (VFCT-8S4, Laboratory
34 Equipments Corp., Japan). The position of the acrylic phantom, as well as the timing of current
35 readout, was computer-controlled using LabVIEW software.

36 We varied the thickness of the acrylic phantom from 7 to 47 mm by adding 10 mm thick

1 acrylic slabs, which allowed us to measure the current values for the different acrylic thicknesses and
 2 thereby obtain the response functions. For CT measurements, we replaced the rectangular phantom
 3 by a cylindrical acrylic phantom 40 mm in diameter. The cylindrical acrylic phantom had a 10 mm
 4 diameter hole at the center to accept iodine tincture thinned by water (30 μm in 10 mm water) and
 5 was mounted on a precision x - θ stage.

7 2.2 Response functions

8 The energy ranges of interest are just above and below the K-edge of iodine. To study the
 9 x-rays energy distribution for tube voltages of 50, 65, and 80 kV, we define six energy ranges as
 10 follows: E_1 , 20–27 keV, E_2 , 28–33 keV, E_3 , 34–39 keV, E_4 , 40–50 keV, E_5 , 51–65 keV, and E_6 ,
 11 66–80 keV. The number of events in each energy range Y_i ($i = 1,6$) and the measured current by each
 12 segment detector I_j ($j = 1,6$) are related by

$$13 \quad \begin{pmatrix} I_1 \\ I_2 \\ \vdots \\ I_6 \end{pmatrix} = \begin{pmatrix} R_{11} & R_{12} & \cdots & R_{16} \\ & R_{21} & \ddots & \\ & \vdots & & \\ & R_{61} & \cdots & R_{66} \end{pmatrix} \begin{pmatrix} Y_1 \\ Y_2 \\ \vdots \\ Y_6 \end{pmatrix}. \quad (1)$$

14 Here, R_{ij} ($i,j = 1,6$) are the response functions. Unfolding Eq. (1) by the SAND II code, the energy
 15 distribution of the incident x-rays Y_i is obtained [6].

16 To obtain response functions that correspond to various acrylic thicknesses, we plotted the
 17 measured current values as a function of acrylic thickness for each segment detector, and fit a
 18 semi-log curve to the data. The semi-log fit allows us to estimate the current values for the acrylic
 19 thicknesses that we did not measure experimentally.

20 For the initial guess of the x-ray energy distribution, the calculated energy distributions Y_1^0
 21 are generated for acrylic thicknesses ranging from 7 to 47 mm in 1 mm steps, and the iodine
 22 thicknesses from 0 to 70 μm in 1 μm steps, using Eq. (2) of Ref. [2]. With the CT image obtained
 23 from the current measurements (e.g., obtained by the segment detector 1) the acrylic thickness d
 24 through which the x-rays passed is calculated, and then this response function for the acrylic
 25 phantom thickness d mm is used in the unfolding process. With the initial guesses of the x-ray
 26 energy distribution for fixed x-rays path length d but changing iodine thickness, an x-ray energy
 27 distribution with the smallest SAND II error is taken as the most probable x-ray energy distribution.

29 2.3 CT images and CT values

30 CT images of 40 mm diameter acrylic phantoms, obtained using the conventional current
 31 measurement method and the ES method, are shown in Fig. 3 for the case of 65 kV x-ray tube
 32 voltage. The profiles at the center of the phantom are shown in Fig. 4 for x-ray tube voltages of 50,

1 65, and 80 kV. When the response function obtained for the acrylic thicknesses corresponds to the
2 x-ray path length, the CT values in the acrylic region become nearly constant, which represents an
3 improvement over previous work [5]. For a tube voltage of 50 kV, the difference in CT values
4 between the iodine and the acrylic regions is nearly the same for the current and the ES CT
5 measurement. In this experiment, the current CT values for tube voltages of 50 and 65 kV tube
6 happened to be nearly the same. The ES CT values, however, stayed nearly constant, independent of
7 the x-ray tube voltage, whereas the conventional current CT suffers from the beam hardening effect.
8 In particular, the ES CT value is twice as big as the current CT value at a tube voltage of 80 kV. This
9 result shows that the ES CT is insensitive to the beam hardening effect, even when the energy
10 information is obtained using the transXend detector.

11 12 3. Conclusion

13 The energy subtraction (ES) method for x-ray CT is shown to be insensitive to the beam
14 hardening effect, which is a distinct advantage over the conventional current measurement CT
15 method. To make the ES CT method practical, the current-mode detector “transXend” was
16 developed, which measures the energy distribution of the incident x-rays. The transXend detector
17 required knowledge of the response functions, which must be obtained as a function to the thickness
18 of the subject through which the x-rays pass. Knowledge of the response functions allows the
19 derivation of the x-ray energy distribution. The path length of the x-rays through the subject under
20 investigation is obtained by conventional current CT, which is always available when using the
21 transXend detector. When using the response functions, which are dependent on the subject
22 thickness, the CT values of the same material become nearly constant.

23 24 Acknowledgment

25 We are grateful to Prof. T. Shoji and Dr. K. Hitomi of the Tohoku Institute of Technology
26 for allowing us to use their CT image reconstruction code. This study was partly supported by a
27 Grant-in-Aid for Scientific Research from the Japan Society for the Promotion of Science.

28 29 References

- 30 [1] R. A. Brooks, G. Di Chiro, *Phys. Med. Biol.*, **21**(1976) 390.
31 [2] I. Kanno, A. Uesaka, S. Nomiya, H. Onabe, *J. Nucl. Sci. Technol.*, **45** (2008) 15.
32 [3] I. Kanno, R. Imamura, K. Mikami, H. Hashimoto, M. Ohtaka, K. Ara, S. Nomiya, H. Onabe, *J.*
33 *Nucl. Sci. Technol.*, **45** (2008) 1165.
34 [4] H. Hirayama, Y. Namito, A. F. Bielajew, S. J. Wilderman, W. R. Nelson, *SLAc-R-730* (2005).
35 [5] I. Kanno, R. Imamura, K. Mikami, H. Hashimoto, M. Ohtaka, K. Ara, S. Nomiya, H. Onabe,
36 *Nucl. Instr. and Meth. Phys. Res.*, **A610** (2009) 325.

1 [6] W. McElroy, S. Berg, T. Crocket, G. Hawkins, AFWL-TR-67-41 (1967).

2

3

4

5

6

7

8

9

10

11

12

13

14

15

16

17

18

19

20

21

22

23

24

25

26

27

28

29

30

31

32

33

34

35

36

1 Figure captions

2

3 Figure 1 Schematic drawing of a transXend detector.

4

5 Figure 2 Schematic drawing of the experimental setup.

6

7 Figure 3 CT images reconstructed using (a) current and (b) energy subtraction data. The x-ray
8 tube voltage was 65 kV.

9

10 Figure 4 CT values for the current and energy subtraction CT at the center of CT images in Fig. 3.
11 The x-ray tube voltages are shown in the figure.

12

13

14

15

16

17

18

19

20

21

22

23

24

25

26

27

28

29

30

31

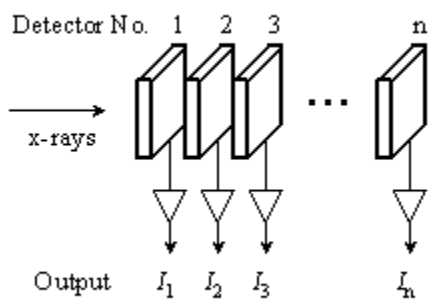
32

33

34

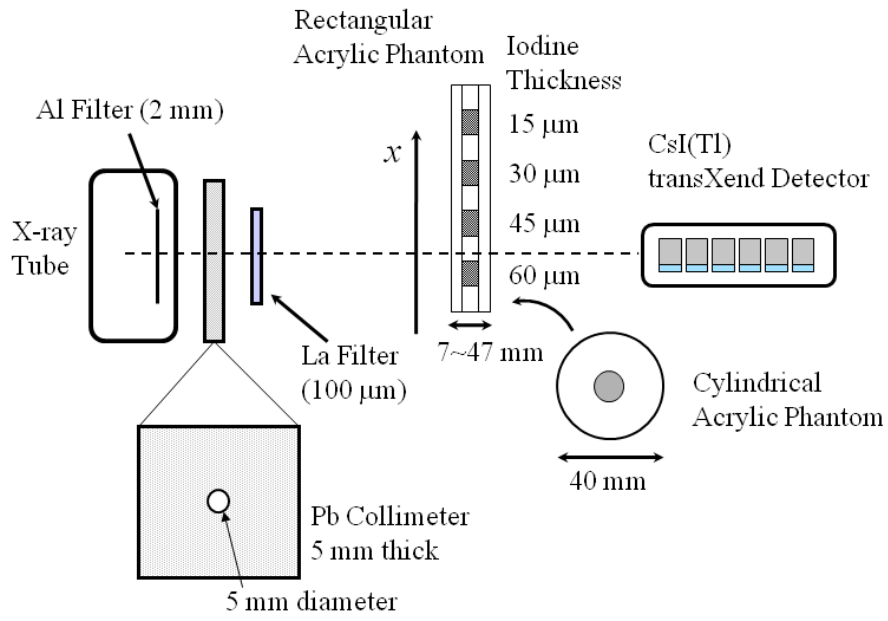
35

36



- 1
- 2
- 3
- 4
- 5
- 6
- 7
- 8
- 9
- 10
- 11
- 12
- 13
- 14
- 15
- 16
- 17
- 18
- 19
- 20
- 21
- 22
- 23
- 24
- 25
- 26
- 27
- 28

Figure 1



2

3

4 Figure 2

5

6

7

8

9

10

11

12

13

14

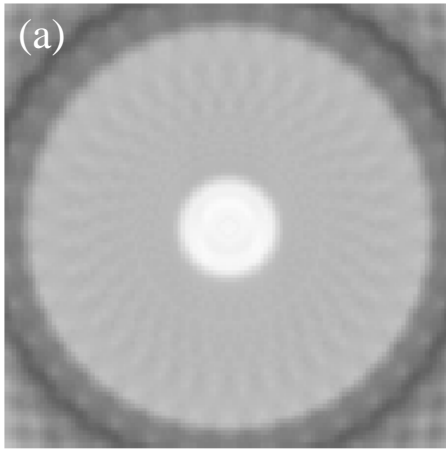
15

16

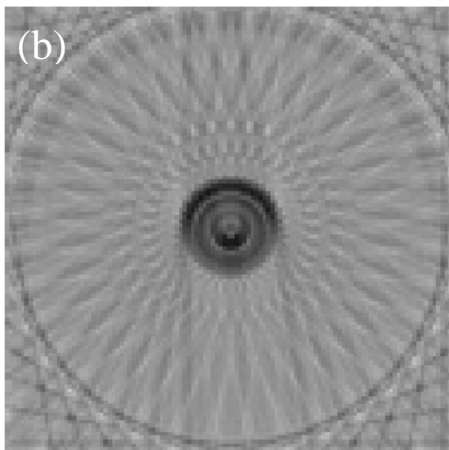
17

18

19



1



2

3

4

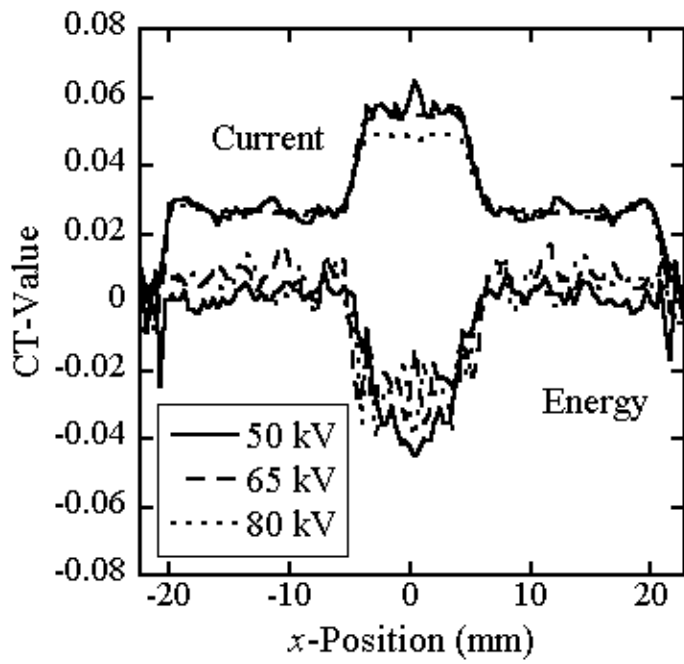
Figure 3

5

6

7

8



- 1
- 2
- 3 Figure 4